OPEN ACCESS

Original research

Mutational signatures define immune and Wnt-associated subtypes of ampullary carcinoma

Ekaterina Zhuravleva,[1] Monika Lewinska ,[1] Colm J O'Rourke,[1] Antonio Pea,[2,3] Asif Rashid,[4] Ann W Hsing,[5] Andrzej Taranta,[1] David Chang,[2] Yu-Tang Gao,[6] Jill Koshiol ,[7] Rui Caetano Oliveira,[8] Jesper B Andersen [1]

► Additional supplemental material is published online only. To view, please visit the journal online (https://doi.org/10.1136/gutjnl-2024-333368).

[1]Biotech Research and Innovation Center (BRIC), Department of Health and Medical Sciences, University of Copenhagen, Copenhagen, Denmark
[2]University of Glasgow, Wolfson Wohl Cancer Research Centre, School of Cancer Sciences, Glasgow, UK
[3]University of Verona, Verona, Italy
[4]Department of Pathology, Division of Pathology/Lab Medicine, MD Anderson Cancer Center, The University of Texas, Houston, Texas, USA
[5]Stanford Cancer Institute and Stanford Prevention Research Center, Department of Medicine, Stanford School of Medicine, Stanford University, Palo Alto, California, USA
[6]Department of Epidemiology, Shanghai Cancer Institute, Shanghai, Shanghai, China
[7]Division of Cancer Epidemiology and Genetics, NIH, Rockville, Maryland, USA
[8]Centro Hospitalar de Coimbra, Universitário de Coimbra, Coimbra, Portugal

Correspondence to
Dr Jesper B Andersen; jesper.andersen@bric.ku.dk

Received 16 July 2024
Accepted 21 November 2024
Published Online First 26 December 2024

To cite: Zhuravleva E, Lewinska M, O'Rourke CJ, *et al*. *Gut* 2025;**74**:804–814.

ABSTRACT

Background and objective Ampullary carcinoma (AMPAC) taxonomy is based on morphology and immunohistochemistry. This classification lacks prognostic reliability and unique genetic associations. We applied an approach of integrative genomics characterising patients with AMPAC exploring molecular subtypes that may guide personalised treatments.

Design We analysed the mutational landscapes of 170 patients with AMPAC. The discovery included 110 tumour/normal pairs and the validation comprised 60 patients. In a tumour subset, we interrogated the transcriptomes and DNA methylomes. Patients were stratified based on mutational signatures and associated with molecular and clinical features. To evaluate tumour and immune cellularity, 22 tumours were independently assessed histomorphologically and by digital pathology.

Results We defined three patient clusters by mutational signatures independent of histomorphology. Cluster 1 (C1) was defined by spontaneous deamination of DNA 5-methylcytosine and defective mismatch repair. C2 and C3 were related to the activity of transcription-coupled nucleotide excision repair but C3 was further defined by the polymerase eta mutational process. C1–2 showed enrichment of Wnt pathway alterations, aberrant DNA methylation profiles, immune cell exclusion and patients with poor prognosis. These features were associated with a hypermutator phenotype caused by C>T alterations at CpGs. C3 patients with improved overall survival were associated with activation of immune-related pathways, immune infiltration and elevated expression of immunoinhibitory checkpoint genes.

Conclusion Immunogenicity and Wnt pathway associations, emphasised by the mutational signatures, defined patients with prospective sensitivity to either immunotherapy or Wnt pathway inhibitors. This emphasises a novel mutational signature-based AMPAC classification with prognostic potential, suggesting prospective implications for subgroup-specific management of patients with AMPAC.

WHAT IS ALREADY KNOWN ON THIS TOPIC

⇒ Classification of patients with ampullary carcinoma (AMPAC) into intestinal and pancreatobiliary histomorphological subtypes has generated debate as to their prognostic associations and therapeutic sensitivities.
⇒ Genomic characterisation of AMPAC supports it as a distinct cancer type rather than intestinal-type AMPAC being more similar to intestinal malignancies or the pancreatic subset being more similar to pancreatic adenocarcinoma.
⇒ Wnt pathway activation mutations (adenomatous polyposis coli, SMAD family member 4, *CTNNB1* and E74-like ETS transcription factor 3) are key drivers in AMPAC but are not exclusively associated with histomorphological subtypes.

INTRODUCTION

Ampullary carcinoma (AMPAC) is a heterogeneous malignancy with origin in the biliary, duodenal and pancreatic epithelial cell layers converging in the ampulla of Vater.[1] Surgically, AMPAC comprises 30% of pancreaticoduodenectomies and 20% of tumour-related obstructions of the common bile duct.[2] The average age at diagnosis ranges from 60 to 70 years old[2] and the incidence rates are estimated at 0.46 and 0.30 per 100 000 for men and women, respectively.[3] Patients with AMPAC are usually diagnosed at an advanced stage with approximately 50% of cases presenting as non-resectable disease.[3] The 5-year relative survival rate is 30%[3] (The Surveillance, Epidemiology, and End Results (SEER) Program: 34.5%–95% CI 33% to 36%) as patients respond poorly to both chemotherapy[4] and adjuvant treatments,[5–7] though significant interpatient survival variability is observed. The taxonomy of AMPAC is stratified into intestinal and pancreatobiliary subtypes based on the anatomical site of origin accompanied by morphological and immunohistochemical annotations. However, the prognostic reliability of these subtypes is debated[2 8] and it remains unclear whether the histomorphological subtypes may respond differently to targeted therapies. Therefore, emphasising patient subgroups with differential prognosis, molecular pathogenesis and sensitivity to specific therapies is required to advance the clinical management of these patients. Detailed molecular analysis of AMPAC remains limited and is often misclassified as other periampullary tumour types.[3]

Recurrent mutations reported in AMPAC[9–11] include common tumour driver genes similar to most gastrointestinal tumours and whereas the prevalence of these mutations has been linked to morphological subtypes[9] none of these genes are subtype exclusive, emphasising that common molecular tumourigenic processes in tumours with unique histomorphology. Activating mutations in

WHAT THIS STUDY ADDS

⇒ We define Wnt pathway suppressor *RNF43* mutations and deletions, recurrent *MYC* amplification and SND1-BRAF fusion as novel candidate drivers potentially involved in AMPAC tumourigenesis.

⇒ We demonstrate the association of Wnt pathway-activating mutations, mutational signatures and global DNA methylation loss as hallmarks of distinct tumourigenic trajectories in AMPAC.

⇒ We use mutational signatures to classify AMPAC into two distinct patient groups. The first group (C1 and C2) is defined by immune exclusion and intermediate immune type tumours characterised by Wnt pathway alterations and suitable for putative Wnt pathway-targeted therapies (β-catenin/TGF-β inhibitors). The second group (C3) is more likely to respond to immune checkpoint inhibitors.

⇒ We demonstrate that signature 1, specifically C>T at CpG sites, causes a hypermutator phenotype that correlates with mutations in Cadherin signalling and WNT pathway genes as well as loss of methylation in a subset of AMPAC tumours.

HOW THIS STUDY MIGHT AFFECT RESEARCH, PRACTICE OR POLICY

⇒ Mutational signature-based classification of patients with AMPAC highlights the urgent need for clinical trials pursuing novel Wnt pathway-targeted therapies in this rare patient demographic.

⇒ Genomic stratification of AMPAC suggests that immune checkpoint inhibitors might be efficacious in a distinct subgroup of patients facilitating precision application of immunotherapy while clinically balancing non-beneficial response to such treatments as evident in other tumour types.

the Wnt pathway which are involved in cancer initiation and progression[12–14] were also shown in AMPAC, irrespective of the morphological subtype.[9 11] However, only a fraction of patients are characterised by Wnt pathway deregulation indicating that the underlying molecular processes in a majority of AMPAC remain elusive.[11]

In this study, we integrated genomic alterations, transcriptome deregulation and DNA methylation profiles in AMPAC. We assessed histomorphological features and immune cell infiltration by digital pathology according to subtypes. We showed that patient subgrouping is based on the impact of mutational signatures representing a combination of mutational patterns arising from distinct mutational processes active in the tumour genomes.[15] This novel signature-based taxonomy divides patients with AMPAC according to association with Wnt pathway alterations, global DNA methylation loss and immune cell infiltration into the tumour prospectively guiding treatment.

MATERIALS AND METHODS

Patient tissue collection

In total, 192 patients with AMPAC were obtained for analysis (figure 1). Within this series of samples, we included 94 tumour/normal pairs for whole-exome sequencing (WES) and 28 matched RNAseq from phs000895.v1.p1[11] with patients of Caucasian (n=88) and Chinese (n=6) origins. Additionally, snap-frozen samples from 16 patients recruited in China between 1997 and 2001 under the Shanghai Biliary Tract Study at the National Institutes of Health (NIH), USA[16] were included. These samples were processed by WES (tumour/normal pairs, n=16), RNAseq (tumour; n=15) and DNA methylation (tumour, n=16). A validation cohort was included comprising a total of 60 AMPAC tumours obtained from Japanese and American patients.[9] Normal bile ducts (n=6)[17] resected from donor patients treated at the Surgical Branch, NIH were used as reference tissues in the DNA methylation analysis. According to the histopathology evaluation of the discovery set (n=110 patients), 53 patients were of the intestinal type, 37 pancreatobiliary and 16 mixed morphology, respectively (the subtype of 4 samples could not be defined). Additionally, 22 Caucasian patients with AMPAC recruited in Portugal were evaluated by histomorphology, immunostaining and digital pathology. The diagnosis was confirmed by independent board-certified pathologists (AR and RCO). All patients demographic and clinicopathological data were anonymised and are summarised in online supplemental tables S1 and S2.

Further details about methods and data processing are given in online supplemental information.

Data availability statement

Data sets relevant to this study are included in the online supplemental information and available at Gene Expression Omnibus (GEO) with accession number GSE159099.

RESULTS

Characterisation of genome alterations in AMPAC

To comprehensively characterise the genomic landscapes of AMPAC, we analysed WES data from 170 patients including 110 tumours with matched germlines in the discovery set and 60 tumours in the validation set (figure 1). We called somatic mutations including single-nucleotide variants (SNVs), short insertion-deletions (indels), copy number (CN) alterations and gene fusions (figure 2A, online supplemental tables S3–S6). In total, we detected 21 268 somatic mutations with 13 201 non-silent SNVs and 3076 non-silent indels in protein-coding genes (online supplemental figure S1A). On average, each patient had 148 somatic alterations per tumour (median 71) consisting of 120 SNVs (median 61) and 28 indels (median 6). Microsatellite instability (MSI) was detected in 6.4% of tumours (figure 2A) which was associated with a significantly lower rate of deletions (on average 10.7 in MSI tumours and 34.7 in microsatellite stable (MSS) tumours, $p<0.01$ t-test) and a higher mutation rate (34.4 mutations per Mb in MSI vs 2.3 in MSS, $p=0.015$ t-test; online supplemental figure S1B) which is comparable to previously reported mutation rates in AMPAC.[9 11] MSI-high tumours were associated with improved overall survival (OS) (Kaplan-Meier $p=0.038$, (online supplemental figure S1C) and enriched for mutations in DNA mismatch repair genes (online supplemental figure S1D) as MSI often is a consequence of mismatch repair deficiency.[18]

Next, we identified 14 common and significantly mutated genes[19 20] including Tumour protein P53 (*TP53*, in 50% of 110 samples), Kristen rat sarcoma viral oncogene homolog (45%), adenomatous polyposis coli (*APC*, 26%), serine-protein kinase (*ATM*, 11%), SMAD family member 4 (*SMAD4*, 10%), E74-like ETS transcription factor 3 (*ELF3*, 9%), AT-rich interactive domain 2 (9%) and phosphatidylinositol-4,5-bisphosphate 3-kinase catalytic subunit alpha (9%) (figure 2B, online supplemental table S7). We also observed recurrent mutations in putative cancer-related genes previously not reported in AMPAC such as dynein axonemal heavy chain 5, activated in prostate cancer protein (*PDZD2*) and Aquaporin 7 (*AQP7*). Mutations in *AQP7* were enriched in Caucasian patients.

To associate observed mutations with clinical features, we performed log-rank tests on patients stratified by the occurrence

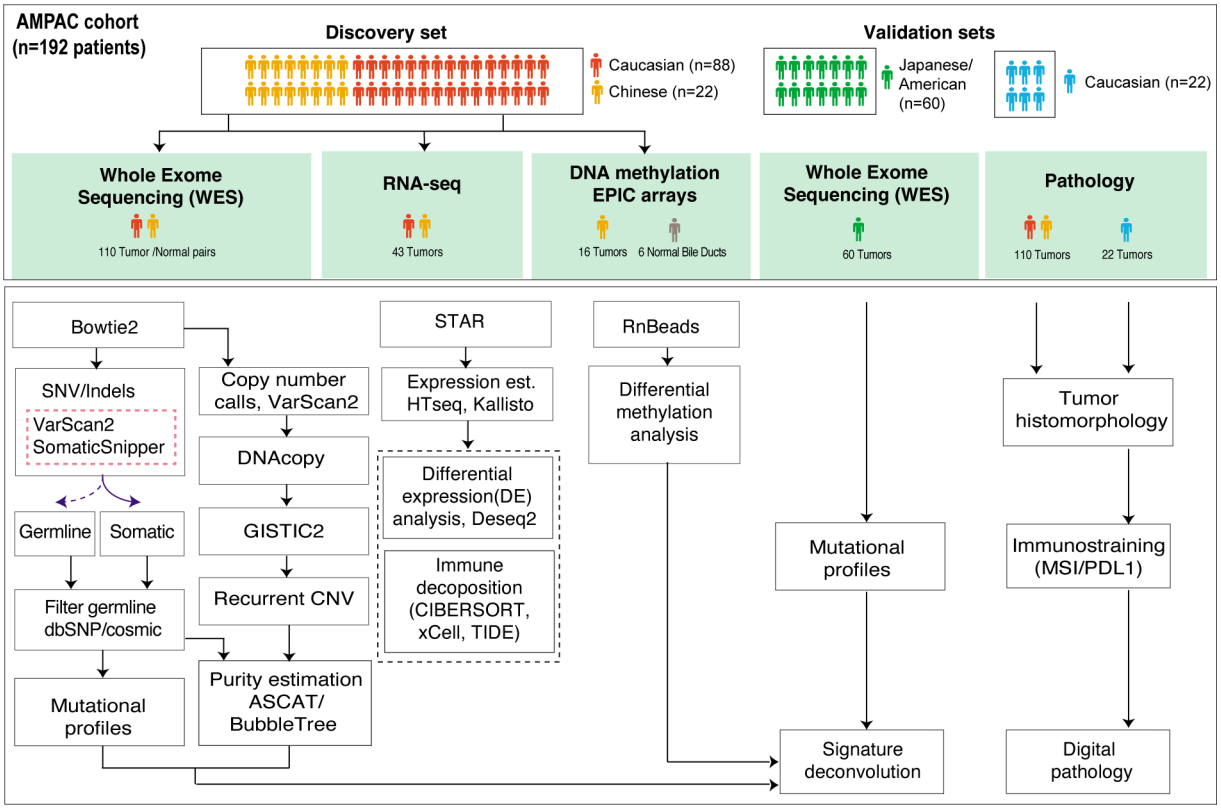

Figure 1 Study data sets and analysis pipeline. Data sets are colour coded in the figure. Whole exome sequencing was performed in the discovery cohort (n=110) and validated by additional n=60 samples. Transcriptome analysis was performed in n=43 cases. DNA methylation was performed in n=16 AMPAC cases with matched WES and RNAseq data sets and additional six normal bile duct samples. Histomorphology evaluations were performed on the discovery cohort (n=110) with additional 22 samples analysed by immunohistochemistry and digital pathology evaluation. AMPAC, ampullary carcinoma; CNV, copy-number variant; dbSNP, single-nucleotide polymorphism database; MSI, microsatellite instability; PDL1, programmed death ligand 1; SNV, single-nucleotide variant.

of recurrent mutations compared with wild type. We observed a significantly shorter survival among patients with mutations in *APC* (p=0.046), *SMAD4* (p=0.032) and trending to significance in *CTNNB1* (p=0.071) and *ELF3* (p=0.068) (online supplemental figure S1E). These genes are associated with the Wnt signalling, re-emphasising the importance of Wnt pathway alterations in AMPAC.[9 11] Also, we showed recurrent alterations in ring finger protein 43 (*RNF43*; mutations observed in 7.3% and deletion in 6.4% of patients, respectively), a negative regulator of Wnt signalling.[21] Importantly, we observed mutational exclusivity between Wnt pathway genes (*APC*, *CTNNB1*) and *ATM* in 46% of patients (p=7.77e−07; online supplemental figure S2A). This mutational exclusivity implies a functional redundancy of the Wnt pathway activating mutations and suggests distinct tumourigenic processes in these tumours. Independent of morphological subtypes, patients with Wnt pathway-activating mutations are associated with shorter survival and upregulation of downstream target genes (online supplemental figure S2B,C). As such, *CTNNB1* is significantly correlated with *MYC* expression in both pancreatobiliary and intestinal subtypes (Pearson r=0.62 and r=0.47, respectively).

Characterisation of recurrent CN gains and losses was associated with significant changes in gene expression between defined groups (figure 2C, online supplemental figure S3A-C, table S4 and S5). Overall, we revealed five large recurrent amplifications (8q24.3, 19p13.3, 11p14.1, 17p13.1, 22q11.23) and two deep deletions (7q22.1, 7q22.3) with a prevalent loss in tumour suppressor genes (14-3-3 epsilon (*YWHAE*), folliculin, nuclear receptor corepressor 1 (*NCOR1*), mitogen-activated protein kinase 4 and RAB GTPase binding effector protein 1; q<0.04). The most prevalent focal gain was in *MYC* (8q24.21) observed in 42.7% of samples. We identified recurrent structural variants in genes with a putative role in tumourigenesis and with consequences directly on their expression (p<0.01, online supplemental table S8). Among these genes, replication protein A1 is deleted in 42.7% of patients with AMPAC. Moreover, we identified nine chromosomal rearrangements forming non-recurrent chimeric fusions in AMPAC (figure 2D). Among these fusions, *SND1-BRAF* was previously reported as recurrent in acinar cell carcinoma with sensitivity to trametinib.[22] However, detected gene fusions were exclusively observed in tumours with already known driver genes and thus, may not function as crucial independent drivers promoting tumour initiation.

To define the main mutated gene networks, we performed enrichment analysis in known pathways and of protein–protein interaction networks as connecting nodes are useful to determine important alterations relevant to AMPAC development beyond common driver genes. We observed an enrichment of mutations prevalent in Wnt signalling and other common cancer-associated pathways (PI3K-Akt, ATM/p53 and MAPK pathways; online supplemental figure S4-D, online supplemental table S9). Overall, we revealed 30 significantly mutated networks linking these to known cellular processes (online supplemental table S10) including transient receptor potential channels, O-glycan processing networks, immune-associated networks (interleukin-10 (IL10) signalling and regulation of IL1 secretion), Wnt

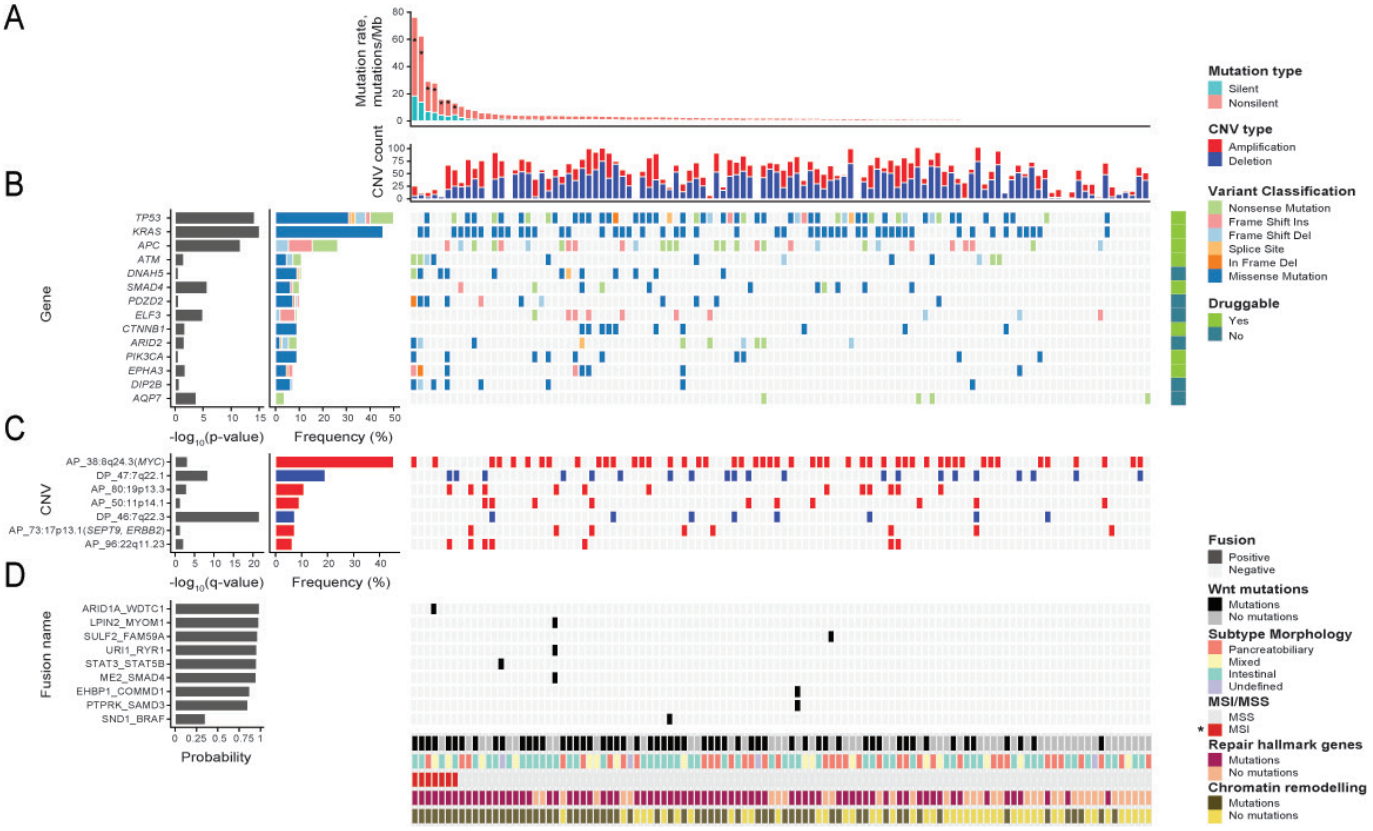

Figure 2 Characterisation of genomic alterations in AMPAC (n=110). (A) Non-silent and silent mutations rate and CNV count (amplifications, deletions). (B) Oncoplot of recurrently mutated genes including druggability annotation. (C) Large-scale recurrent amplifications and deletions defined with GISTIC2. (D) Detection of non-recurrent fusions (genes in fusion and breakpoints) in AMPAC. AMPAC, ampullary carcinoma; APC, adenomatous polyposis coli; AQP7, Aquaporin 7; ARID2, AT-rich interactive domain 2; ATM, serine-protein kinase; CNV, copy-number variant; DNAH5, dynein axonemal heavy chain 5; ELF3, E74-like ETS transcription factor 3; GISTIC2, Genomic Identification of Significant Targets In Cancer; KRAS, Kristen rat sarcoma viral oncogene homolog; MSI, microsatellite instability; MSS, microsatellite stable; PDZD2, activated in prostate cancer protein; PIK3CA, phosphatidylinositol-4,5-bisphosphate 3-kinase catalytic subunit alpha; SMAD4, SMAD family member 4; TP53, Tumour protein P53.

signalling and extracellular matrix and cell adhesion (online supplemental figure S4B–D).

Mutational signatures in AMPAC define molecular subtypes of patients

The mutational profiles of 103 samples were decomposed to mutational signatures by non-negative matrix factorisation[23] and subjected to hierarchical clustering. Mutational signature analysis revealed three patient subclusters (figure 3A). Cluster 1 (C1) was characterised by prevalent signature S1 associated with COSMIC signatures spontaneous deamination signature S1 (SBS1) (cosine=0.99) of spontaneous or enzymatic deamination of 5-methylcytosine and mutation profile of C->T at NCG context (N, any base) as well as SBS6 (cosine=0.96) of defective DNA mismatch repair commonly found in MSI-positive tumours (figure 3B, online supplemental tables S11–S13). Consistent with this, we observed enrichment of MSI in C1 (Fisher test, p<0.0004). C2 was associated with signatures S1 and S2 with S2 corresponding to SBS40 (cosine=0.86) of unknown role and SBS5 (cosine=0.79) which is associated with major damage to adenine on the untranscribed strand and activity of transcription-coupled nucleotide excision repair (NER). C3 was characterised by a prevalent signature S3 corresponding to SBS5 (cosine=0.78) and SBS9 (cosine=0.77), a signature of mutational processes induced during replication by polymerase eta as part of somatic hypermutation in lymphoid cells.[24]

To investigate if mutational signatures differed in their generation time across clusters, we estimated the cancer cell fraction (CCF) for each mutation and repeated the signature deconvolution of signatures S1–3 separately on clonal (CCF>=0.5) and subclonal (CCF<0.5) mutations, respectively. Signature S1 predominantly impacted clonal mutations across all clusters (C11: p=0.027; C2: p=0.0027; C3: p=0.0062) suggesting that mutations associated with S1 may arise early during tumourigenesis (online supplemental figure S5A). In contrast to S1, signature S3 exerted greater impact on subclonal mutations compared with C1 (p=0.026) and C2 (p=0.029). Signature S3 was more prominent in cluster 3 patients and no significant difference was observed in its impact between clonal and subclonal mutations. The mutational clonality suggests that S3 mutational processes may occur continuously during tumour evolution in C3 but not in C1 and C2 tumours where signature S3 mutation-timing is shifted to late tumourigenic events resulting in influence from subclonal mutations.

Next, we compared mutational signature-associated clusters with clinical and molecular features. We observed no significant association of the mutation rate, age or distinct morphologies between clusters. However, we observed a positive association between C3 and signature S3 with the total mutation burden (TMB) across MSS tumours in a regression model (r^2=0.25, p=1e−06, only tumours with>30 mutations are considered, n=87 samples) (online supplemental figure S5B–D).

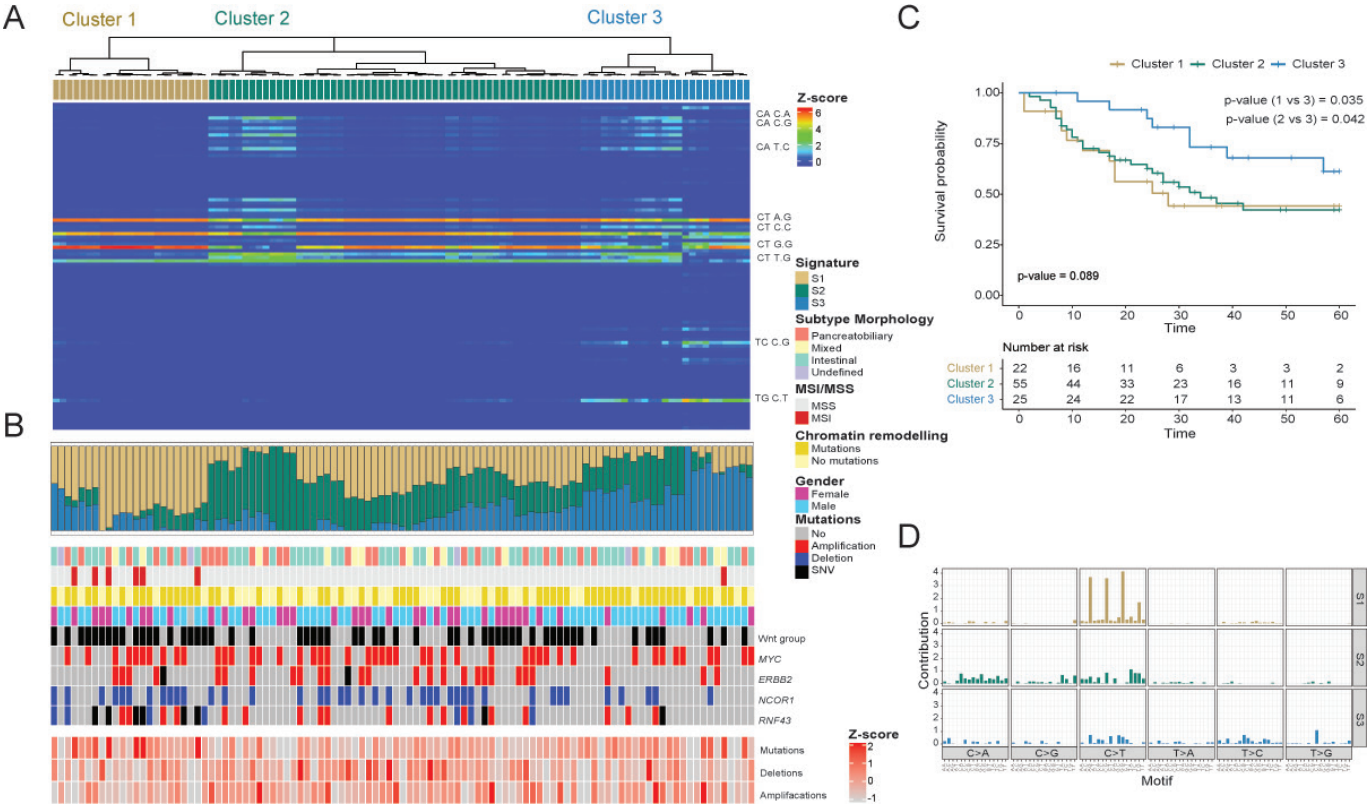

Figure 3 Mutational signature-associated clusters in AMPAC (n=103). (A) Normalised three-nucleotide mutational frequency profiles. (B) Relative mutational signature contribution. (C) Kaplan-Meier analysis of overall survival between clusters. (D) Profiles of decomposed mutational signatures S1, S2 and S3. AMPAC, ampullary carcinoma; MSI, microsatellite instability; MSS, microsatellite stable; NCOR1, nuclear receptor corepressor 1; RNF43, ring finger protein 43; SNV, single-nucleotide variant.

Also, we observed an association of clusters with OS with C3 patients having the best prognosis compared with C1 and C2 (p=0.035 and p=0.042 for pairwise comparison and given clinical similarity between patients in clusters 1 and 2, p=0.031 for C3 vs C1+C2, respectively) (figure 3C). Multivariate analysis by Cox proportional hazards regression modelling confirmed signature clusters to be significantly associated with survival (p=0.011) when considering other relevant features (age, gender, ethnicity, MSI status, morphological subtypes and mutational status of the Wnt pathway genes). We show a significantly higher amount of *NCOR1* and *RNF43* alterations (SNVs and/or deletions) in C1 and C2 (Fisher p<0.05 and p<0.0001, respectively) and *ERBB2* amplifications in C2 (Fisher p<0.05), (figure 3B). Importantly, Wnt pathway mutations were enriched in C1 and low in C3 corresponding to patients with the best prognosis (Fisher test p<0.05, figure 3B). In the validation set, we also observed a significant enrichment of Wnt pathway alterations in samples with a high proportion of signature S1 compared with low S1 (Fisher test p<0.05) (online supplemental figure S6A) and a significantly higher fraction of characteristic S1 C>T mutations (hypermutator phenotype) at CpGs in C1 and 2 (online supplemental figure S6B–D).

To assess the functional dependency of Wnt pathway mutations and thus the potential targetability associated with mutational signatures in AMPAC, we evaluated the genome-wide gene-essentiality by loss-of-function screening (DepMap). In this analysis, we considered all biliary tract cancer (BTC) cell lines to relate the relative impact of individual signatures and observed a functional effect of *CTNNB1* depletion on proliferation significantly associated with Wnt pathway mutated cell lines (online supplemental figure S7). Importantly, the observed *CTNNB1*-dependency was associated with high signature S1 in BTC models (relative S1 impact≥0.3) but not S1 low, resembling our AMPAC patient grouping with Wnt pathway activation.

Mutational signature-defined subtypes exhibit distinct immune infiltrate profiles

To decipher the distinct pathobiological profiles underlying mutational signature-associated clusters, we performed differential transcriptomics and functional Gene Set Enrichment Analysis (GSEA) annotation between clusters. We identified 1001 differently expressed genes in total (figure 4A,B) with upregulation of a set of immune-related pathways in C3 compared with C1 and C2 (figure 4C, online supplemental tables S14–S16). These are pathways uniquely associated with lymphocyte processes such as natural killer (NK) cell-mediated cytotoxicity (p<0.005), Th17 cell differentiation (p<0.005), T-cell receptor signalling (p<0.005) as well as Th1 and Th2 cell differentiation (p<0.009).

Considering the enrichment of immune-related gene sets in C3, we investigated the immune cell infiltration in AMPAC by cellular deconvolution (online supplemental figure S8A, table S17). We identified significantly different immune cell populations of CD8+T, naive B, NK and T follicular helper cells (analysis of variance p<0.05) between clusters as expected with a significant association of lymphocyte infiltration in C3. To further investigate the association between specific mutational signatures and the immune landscape, we tested the association of signature abundance to the immune cell parameters. The

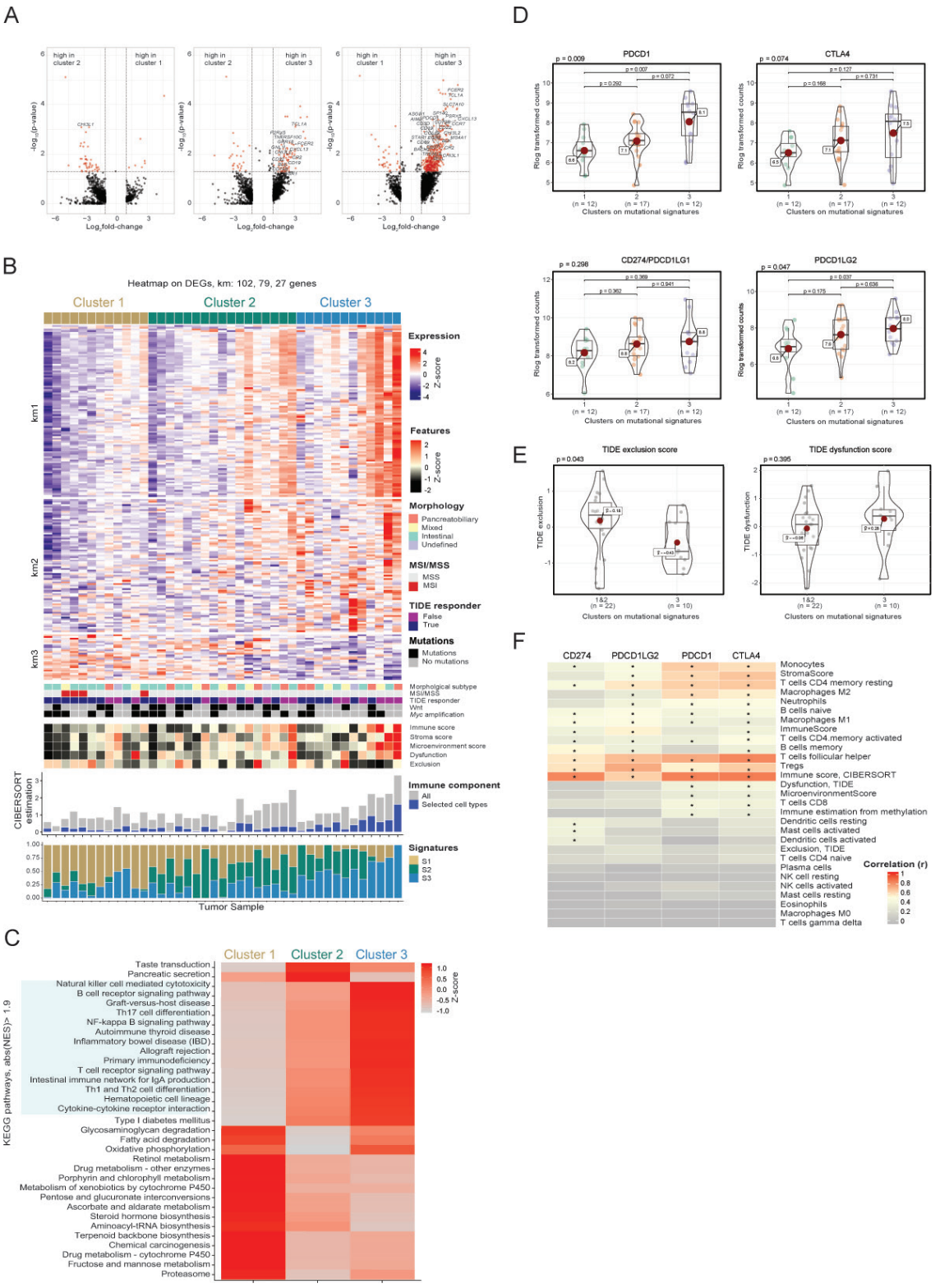

Figure 4 Association of mutational signature-associated clusters with immune parameters (n=43). (A) Volcano plot of differently expressed genes between clusters. Genes from CIBERSORT lm22 immune signatures are highlighted. (B) Heatmap of differentially expressed genes deregulated between clusters. (C) GSEA analysis results, pathways with absolute normalised enrichment score (NES)>1.9 and p.adj<0.05 in at least one pairwise comparison between clusters. Mean expression of all genes in leading edge for each pathway is taken to represent the direction of deregulation between clusters, z-scored. (D) *CTLA-4*, *PDCD1*, *PDCD1LG1*, *PDCD1LG2* gene expression across clusters. (E) Boxplot on TIDE exclusion and dysfunction scores estimation. Only samples with clear morphology were considered and normalisation procedure were made to each morphological group average. C1 and 2 were joined because of samples size. (F) Pearson correlation values between immune parameters and AMPAC clusters. Immune cell type absolute estimation was performed using CIBERSORT. AMPAC, ampullary carcinoma; DEG, differentially expressed genes; MSI, microsatellite instability; GSEA, Gene Set Enrichment Analysis; MSS, microsatellite stable; NK, natural killer; PDCD1, programmed cell death protein 1; PDCD1LG2, programmed cell death 1 ligand 2; TIDE, Tumor Immune Dysfunction and Exclusion.

immune cell content, stromal and microenvironment scores were positively correlated with the relative abundance of signature S3 (Pearson r>0.43, p<0.01) and negatively correlated with T cell exclusion (r=−0.34, p=0.03, TIDE; online supplemental table S18). As polymerase eta-associated mutational processes (S3) may be implicated in somatic immunoglobulin (Ig) gene hypermutation in B cells, we assessed the Ig mutational frequency in genes across clusters and observed no significant differences across MSS samples (online supplemental figure S8A).

Next, we evaluated by immune and histomorphological stains an independent set of 22 AMPACs showing membranous beta-catenin staining in 100% of cases, E-cadherin in 50% and MSI (MLH1, MSH2, MSH6 and PMS2) MMR defects in five tumours (22.7%). MSI positivity is more frequent in patients without metastatic lymph nodes (online supplemental figure S9A, table S19). Still, all tumours were negative for programmed death ligand 1 staining both in the tumour and peritumourous cells. To evaluate the spatial tumour and immune cellularity, we analysed the H&E sections using digital-guided pathology. The cellularity was comparable between histomorphological subtypes (pancreatobiliary or intestinal) (online supplemental figure S9B). Therefore, we sought to assess differences in tumour-infiltrating lymphocytes (TILs) and the cancer cell composition between subtypes. Neighbourhood analysis revealed two regions with clear differences. Region 1 (R1) showing a low density of cancer cells and an increased number of lymphocytes in the tumour periphery whereas R2 was characterised by high tumour cell density (online supplemental figure S9C). When analysing the TIL:tumour cell ratio, intestinal-type tumours showed a significantly higher lymphocyte density in R1 (intestinal (median 6.89, IQR 10.93–5.22) vs pancreatobiliary (5.11, IQR 5.97–4.08), p=0.03) and lower median ratio in R2 (intestinal (0.41, IQR 0.49–0.31) vs pancreatobiliary (0.51, IQR 0.61–0.40), p=0.04) compared with pancreatobiliary-type tumours (online supplemental figure S9D) suggesting that more TILs may have infiltrated deeper (R2) in the pancreatobiliary subtype tumours.

To infer checkpoint inhibitor therapy potential based on the mutational signature-associated clusters, we investigated signatures of cytotoxic T-cell dysfunction and exclusion status[25] and the expression of immune inhibitory checkpoint genes and their ligands. We observed increased immune exclusion potential across joined C1 and 2 compared with C3 (p=0.043) but no significant difference in T cell dysfunction (figure 4E). Furthermore, we uncovered elevated expression of programmed cell death protein 1 (p=0.007) and the ligand programmed cell death 1 ligand 2, *PDCD1LG2* (p=0.037) (figure 4D) in C3 versus C1. We also observed a significant correlation of *PDCD1LG2* and *CTLA4* expression with immune cell components (Pearson r>0.4, p<0.01) (figure 4F). Indeed, high immune cell infiltration in C3 may explain why these patients have a better prognosis and suggest a likelihood of response to immunotherapy.

Altered DNA methylation profiles in AMPAC cluster with mutational signatures

To characterise the genome-wide DNA methylation landscapes in AMPAC, we profiled 16 patients with remaining DNA. First, we performed unsupervised hierarchical clustering and principal component analysis on the most variable probes and regions (promoters, genes and enhancers), (figure 5A, online supplemental tables S20 and S21). These analyses identified two subgroups with significant separation of tumours by clusters (on mutational signatures and Wnt pathway alterations (Fisher tests p=0.03 and p=0.03, respectively)) highlighting a significant involvement of prominent DNA methylation differences in the mutational signature-defined AMPAC clusters and distinct in Wnt pathway activation.

Next, aberrant DNA methylation was assessed in C1 and 2 versus C3 (C1 and C2 were combined due to their similarities in subsequent analyses), analysing ratios of probe methylation across regions defined by the relation to genes and CpG islands (figure 5B, online supplemental tables S22–S24). We observed more probes with higher methylation in C3 compared with C1 and 2 across all genomic regions with a major difference in the open sea and CpG shelf areas ($\log_2$Ratio>4.8). CpG islands showed the least methylation disproportion ($\log_2$R=0.84). To further compare DNA methylation between C1 and 2 and C3, we considered methylation levels in 5 kb tiling windows across the genome. We observed a significant loss in DNA methylation in C1 and 2 compared with C3 using normal bile ducts as control (figure 5C) (mean methylation estimates 0.61 in C1 and 2 and 0.69 in C3 and normal bile ducts, t-test p<2.2e-16). Interestingly, we observed a significantly higher proportion of cytosine mutations in clusters C1 and C2 compared with C3 within the same 5 kb regions with a 2.73-fold increase in the mean cytosine mutation fraction across exome tiling windows (t-test p<2.2e-16) (figure 5D). This finding suggests that the effect of spontaneous cytosine deamination (signature S1) which typically targets methylated cytosines, is not directly correlated with an increased presence of methylated cytosines across the different clusters. Moreover, we observed an anticorrelation between the fraction of cytosine mutations and DNA methylation in both clusters (Pearson r=−0.16 in C1 and 2; r=−0.337 in C3, p<2.2e-16 and r=−0.297 across both clusters with p<2.2e-16). As such, C>T mutations in the CpG context and the fraction of methylated cytosines within genes separate C1 and 2 from C3 (figure 5E), showing a significant association between C>T at CpG hypermutator phenotype with loss of methylation and moreover with a set of recurrently altered genes (figure 5F–H). Indeed, C>T at CpG hotspot mutations were observed in two driver genes (*APC* and *TP53*), both predicted to have mutations of clonal origin, suggesting these are early AMPAC events. Interestingly, over-representation analysis including genes affected by C>T at CpGs in C1 and 2 showed significant segregation of these mutations in Cadherin (fold enrichment=4.17; FDR<0.01) and Wnt pathway (fold enrichment=3.26; FDR<0.01) signalling with a majority of these mutations being of clonal nature.

To evaluate the transcriptional programmes associated with the aberrant DNA methylation in AMPAC, we estimated changes of expression associated with promoter, enhancer and gene body methylation to the corresponding genes. Out of 25 184 genes, a total of 19 106 genes (75.8%) were significantly associated with methylation either in promoters or enhancers by probe/region. Of them, 8265 also showed a positive association between gene body methylation and expression (online supplemental figure S10A). Next, we focused on genes with the most variable expression, selecting promoters, gene body and enhancer regions with a high correlation between gene expression and DNA methylation (online supplemental figure S10B, table S25). We grouped genes into seven classes depending on whether they were regulated by methylation on promoters, enhancers or gene bodies alone or in combination (figure 6A). Subsequently, we annotated 402 differentially methylated regions (DMR) between clusters (figure 6B), with the majority of DMRs (88.8 %) being hypermethylated in C3. On the contrary, the hypomethylated regions in C3 affect CpG islands (35 regions) predominantly in promoters (27/35 regions). Interestingly, the most abundant class of methylated regions in C3 is enhancers which are associated with gene

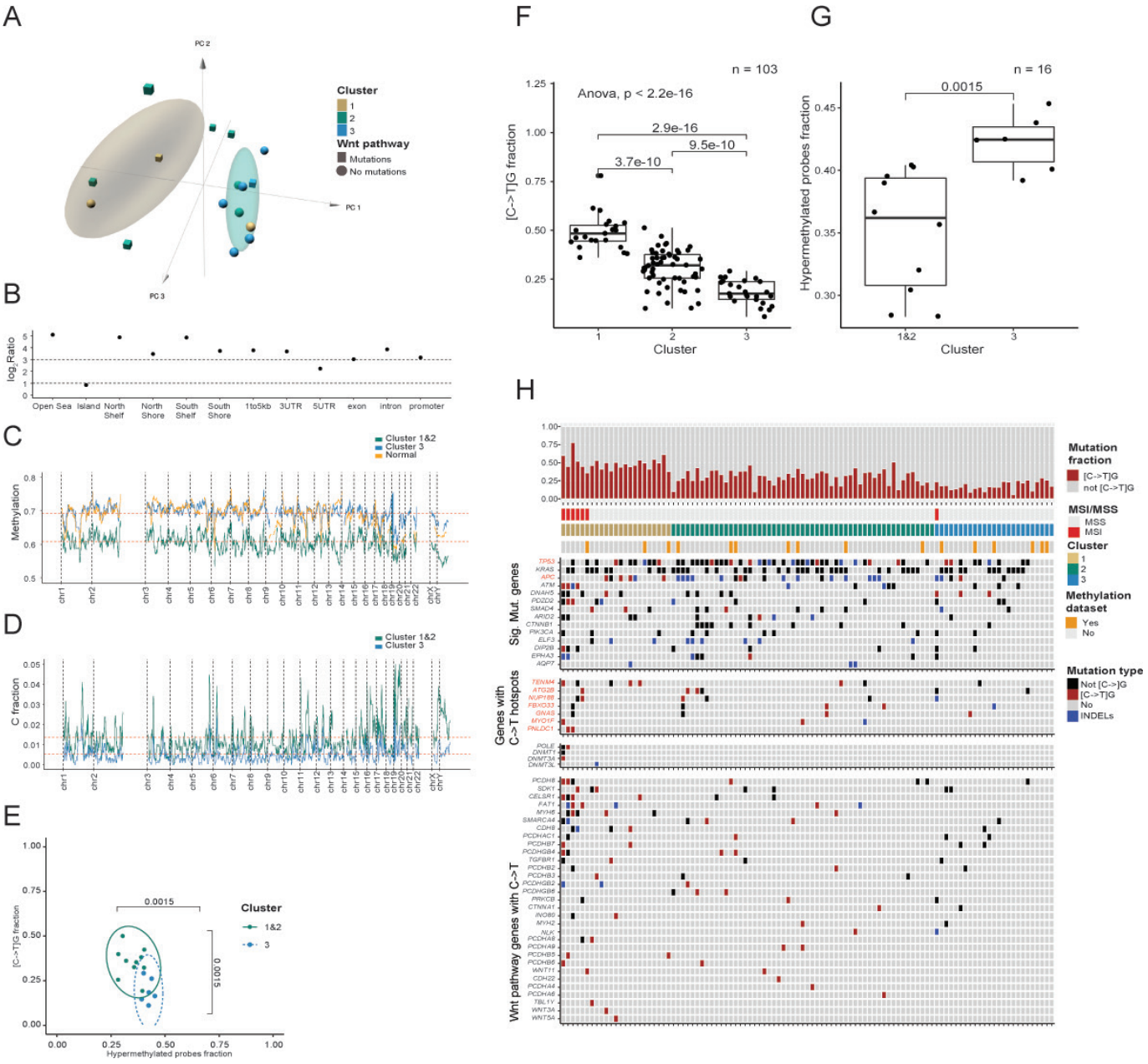

Figure 5 DNA methylation alterations in AMPAC genomes (n=16). (A) Principal component analysis on 10 000 methylation probes with highest variance in the data set. Ellipses are drawn on groupings of samples in hierarchical clustering based on 1000 regions and 10 000 most variable probes. (B) Log_2 Ratios between numbers of probes with higher methylation in C3 compared with C1 and 2 to probes with lower methylation in C3 compared with C1 and 2. Only probes with p value for difference between clusters were considered. Positive value in Log_2 scale indicates increased methylation in corresponding regions in C3. (C) Loss of global methylation in C1 and 2 compared with C3 plotted as roll mean statistics on 1000 5 kb tiling windows. Normal bile duct data is used as control. (D) Proportion of mutated cytosines, normalised by CG content and plotted as roll mean statistics on 1000 5 kb tiling windows. (E) Separation of C1 and 2 and C3 based on the normalised fraction of (C->T)G mutations (signature 1) to all mutations and the hypermethylated cytosine fraction across genes. (F) Normalised fraction of (C->T)G mutations to all mutations across clusters. (G) Normalised fraction of hypermethylated cytosine fraction in gene regions across C1 and 2 versus C3. (H) (C->T)G mutations across genes. Genes with recurrent hotspots are coloured in red. Wnt pathway (C->T)G alterations are over-represented in clusters 1 and 2. AMPAC, ampullary carcinoma; ANOVA, analysis of variance; APC, adenomatous polyposis coli; AQP7, Aquaporin 7; ARID2, AT-rich interactive domain 2; ATM, serine-protein kinase; DNAH5, dynein axonemal heavy chain 5; ELF3, E74-like ETS transcription factor 3; KRAS, Kristen rat sarcoma viral oncogene homolog; MSI, microsatellite instability; MSS, microsatellite stable; PDZD2, activated in prostate cancer protein; PIK3CA, phosphatidylinositol-4,5-bisphosphate 3-kinase catalytic subunit alpha; SMAD4, SMAD family member 4; TP53, Tumour protein P53.

expression regulation alone (97 enhancers, 27.2%) and in combination with promoter regions (69 promoters, 19.3%).

To investigate the functional effects of aberrant DNA methylation between clusters, we performed an over-representation analysis on genes regulated by DNA methylation (figure 6C, online supplemental table S26). Overall, 435 genes were upregulated in C3 including non-coding RNAs and pseudogene transcripts (online supplemental table S10C) as well as 192 genes

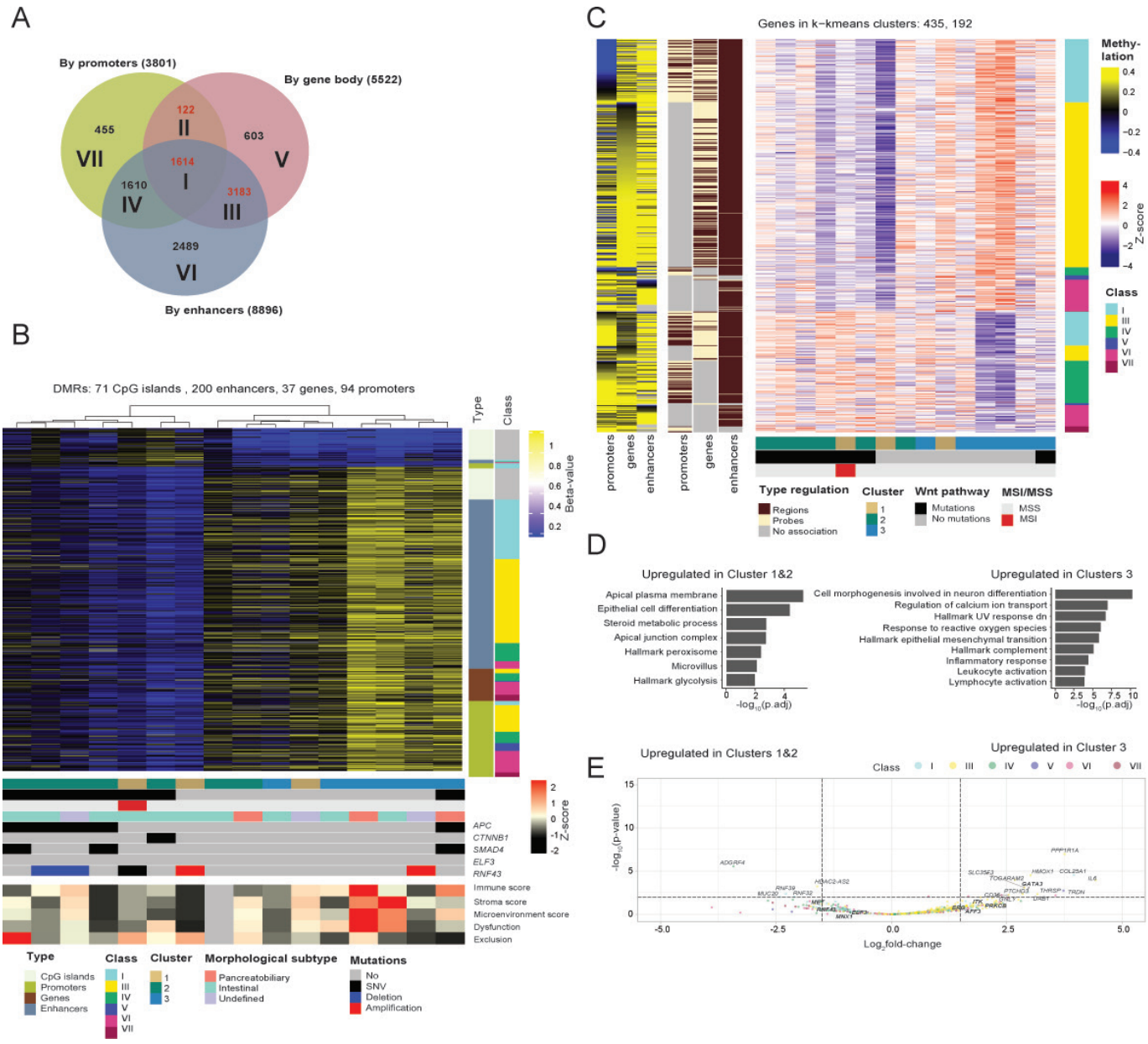

Figure 6 DNA methylation alterations associated with gene expression in AMPAC (n=16). (A) Venn diagram on the numbers of genes with variance of expression above median and with significant association to promoters, enhancers and gene body methylation. (B) Top differently methylated regions (DMR) between C1 and 2 and C3 (402 regions). (C) Expression of genes associated with methylation changes in regions between C1 and 2 and C3. (D) Over-representation analysis of genes regulated by methylation changes. (E) Volcano plot of genes regulated by methylation between C1 and 2 and C3. Genes with absolute logFC>1.5 and adjusted p<0.01 are labelled, oncogenes and tumour suppressor genes are labelled in bold. AMPAC, ampullary carcinoma; APC, adenomatous polyposis coli; ELF3, E74-like ETS transcription factor 3; MSI, microsatellite instability; MSS, microsatellite stable; SMAD4, SMAD family member 4; SNV, single-nucleotide variant.

upregulated in C1 and 2. In C3, we predominantly observed the upregulation of immune pathways (inflammatory response and lymphocyte activation) and the hallmark of genes encoding components of the complement system (figure 6D,E). These findings are consistent with our transcriptome-based predictions of increased immune infiltrates in C3. Interestingly, we also observed DNA methylation-associated downregulation of UV response genes in C1 and 2.

To corroborate the association between immune infiltration and DNA methylation, we applied the immune-component estimation algorithm from the RnBeads package to our methylation data and compared this analysis to the RNAseq-derived immune estimations. Indeed, this highly correlated with expression-derived estimates of tumour immune composition, increasing confidence in the decomposition procedures (r=0.92, p<0.2e-5 for CIBERSORT and r=0.8, p<0.001 for xCell) (online supplemental table S18).

DISCUSSION

Integration of AMPAC genomes, transcriptomes and DNA methylomes demonstrates the potential of mutational signatures deconstructed from tumour exomes to define biological-relevant and clinically distinct patient groups with distinct molecular

subtypes. This molecular-based taxonomy may be relevant in designing personalised therapies for patients with AMPAC including future studies testing the clinical utility of immunotherapy and/or targeting the Wnt pathway (for example, β-catenin/TGF-beta inhibition). We have shown a unique association between frequent Wnt pathway alterations, DNA methylation loss and low immune cell infiltration in clusters C1 and C2. In contrast, C3 highlights tumours with extensive T-cell infiltration and dysfunction. Notably, the molecular subtypes are independent of the previously reported morphological classification and agree with recent studies emphasising the limitations of AMPAC histomorphology in patient stratification.[2 9 11]

Patients C1 and C2 show a high impact of SBS1 and intermediate DNA methylation levels at multiple loci across genomes. The impact of the clock-like signature S1[26] was not associated with age suggesting a higher accumulation of mutations due to an increased proliferation rate in these tumours or deficiency in the mechanisms repairing deaminated cytosines. In fact, DNA methylation loss can be associated with increased proliferation[27 28] following failure of DNA methylation maintenance during replication. Therefore, the anticorrelation between the processes of cytosine deamination and DNA methylation loss in AMPAC supports the simultaneous activity of these processes and their association with increased tumour cell proliferation. C1 and C2 are characterised by significant enrichment of Wnt pathway-activating alterations including *APC*, *CTNNB1, ELF3, SMAD4, RNF43*.[9 11] We highlight *RNF43,* as this gene was not previously associated with Wnt pathway activation in AMPAC. Indeed, these tumours are characterised by high immune exclusion which may relate to the aberrant Wnt pathway activation in these patients. Wnt/*CTNNB1* mutations have been shown to translate to immune evasion through immune cell exclusion in hepatocellular carcinoma[29] relating to resistance of ICB.[30] Indeed, Wnt/*CTNNB1* mutations prevent antitumour immunity in patients with melanoma.[31] On the contrary, in patients with renal cell carcinoma with high tumour immune cell infiltration present a worse prognosis and are predicted to respond poorly to ICB therapy because of high cytotoxic T-lymphocyte dysfunction.[25] Interestingly, C1 and C2 resembled colorectal cancers in the accumulation of mutations caused by C>T at CpG sites including hotspots in *APC* and *TP53*.[32] In contrast to colorectal cancers, we did not observe a positive correlation between highly methylated cytosines and the cytosine deamination mutational fraction. This observation may be either related to the efficiency of cytosine deamination repair or a change in the proliferation rate. Importantly, we observed a significant enrichment of Wnt pathway genes across genes affected by C>T at CpG in signature S1 hypermutator phenotype grouping and the clonality of these events suggests an early generation.

Proteins downstream of the Wnt pathway, such as c-Myc, are associated with global methylation changes in previous studies[33] similar to what we observed in our AMPAC data. Indeed, *MYC* is considered a super transcription factor, regulating major parts of the genome,[34] including epigenomic deregulation[35] and immune privilege.[36] The characteristic global DNA methylation loss associated with C1 and 2 was also shown pancancer to be independently related to tumour immune evasion and a higher likelihood of beneficial response to checkpoint therapy response than TMB.[27] Therefore, we highlight a novel link between DNA methylation loss and Wnt pathway activation associated with immune evasion in AMPAC. Interestingly, S1 signature high impact was associated with an increased effect of *CTNNB1* depletion on the proliferation in Wnt pathway mutated cancer cells suggesting a key role of WNT inhibition. This highlights a need to investigate the clinical implications of mutational signatures to predict drug response.

Independent of Wnt pathway activation, a second oncogenic path in C3 tumours is driven by mutational processes associated with cosmic signatures SBS5 and SBS9. The SBS5 is associated with the activity of transcription-coupled NER and SBS9 is coupled to the error-prone polymerase eta.[15] Moreover, C3 showed a lower impact of SBS1 which was shown to be negatively correlated to immune features such as immune cell infiltration and immune checkpoint gene expression across cancers.[37] In contrast, AID/APOBEC deamination signature activity was previously shown to be significantly correlated to immune cell infiltration.[37] As such, the polymerase eta mutational process is associated with AID deamination-related mutations in non-solid cancers.[38] Though, its presence in solid tumours remains controversial, the motif WRCY (where W=A/T; R=A/G; Y=C/T) which is reminiscent of the deamination of cytosines was observed as part of our signature S3 profile. Interestingly, mutational signatures grouping in pancreatic ductal adenocarcinoma have defined an association between double-stranded break (DSB) repair and mismatch repair in subtypes with the increased expression of antitumour immunity.[39] The observed NER deficiency in AMPAC may be a cause of increased immunity due to NER-associated DSBs.[40] Both SBS5 and SBS9 target transcriptionally active genes[41] and thus might be associated with increased presentation of neoantigens and tumour immune cell infiltration.[39 42] Interestingly, from the signature analysis of clonality signature S3 (SBS5 and SBS9), the related mutations in C3 were not only prevalent but also suggested a continuum in tumour evolution with mutations proportionate in both clonal and subclonal groups compared to C1 and C2.

Although the sample size is limiting, subclustering and multiple comparisons require interpretation with caution. Besides, the integrative genomics study was not designed to investigate the utility of immunotherapy and thus warrants future clinical assessment in a well-powered cohort. This study indicates that mutational signatures are associated with distinct molecular subtypes and prospective therapeutic sensitivities in AMPAC. AMPAC showing immune evasion is associated with Wnt pathway activation and thus may benefit from Wnt pathway-targeted therapy[43] including small-molecule inhibitors for β-catenin.[44 45] Moreover, the immunogenic subtype C3 may be patients suited for ICB, highlighting for the first time the relevance of immunotherapy in AMPAC.

X Antonio Pea @antonio pea and Jesper B Andersen @jaboeje

Acknowledgements The authors thank the participating patients, families and clinical personnel. The study is in part based upon data generated by the TCGA Research Network: https://www.cancer.gov/tcga. This publication is based upon work from COST Action Precision-BTC-Network (CA22125), supported by COST (European Cooperation in Science and Technology; www.cost.eu).

Contributors JBA is responsible for the overall content as guarantor. EZ and JBA designed the study. EZ, CJO'R, AP, RCO, DC and AT generated and analysed data. AWH, Y-TG, JK and JBA recruited patients, provided samples and data. AR, RCO and AP performed histopathological evaluations. EZ, ML, CJO'R and JBA interpreted data and wrote the manuscript. All authors revised and approved the manuscript.

Funding The laboratory of JBA is supported by the Novo Nordisk Foundation (14040, 0058419, 220C0074956), Danish Cancer Society (R98-A6446, R167-A10784, R278-A16638, R368-A21455), Independent Research Fund Denmark for Medical Research (4183-00118A, 1030-00070B), NEYE Foundation and AMMF-The UK Cholangiocarcinoma Charity (EU/2022/212).

Competing interests JBA declares consultancies for Flagship Pioneering, Seald, QED Therapeutics and AstraZeneca. JBA has received funding from the Incyte Corporation (EU-DK-ST-21122) but not related to this study.

Patient and public involvement Patients and/or the public were not involved in the design, or conduct, or reporting, or dissemination plans of this research.

Patient consent for publication Not applicable.

Ethics approval The Danish Regional Ethics Committee (protocol H-4-2015-FSP no. 15014207), the US National Cancer Institute (IRB Protocol #OH97CN028) and CHUC, Portugal (OBS.SF.157-2021) approved the use of patient material in this study. Written informed patient consent was obtained in accordance to regional regulations.

Provenance and peer review Not commissioned; externally peer reviewed.

Data availability statement Data are available in a public, open access repository. Data sets relevant to this study are included in the supplementary information and available at GEO with accession number GSE159099.

ORCID iDs
Monika Lewinska http://orcid.org/0000-0002-5275-992X
Jill Koshiol http://orcid.org/0000-0002-3832-6204
Jesper B Andersen http://orcid.org/0000-0003-1760-5244

REFERENCES

1 Adsay V, Ohike N, Tajiri T, *et al*. Ampullary region carcinomas: definition and site specific classification with delineation of four clinicopathologically and prognostically distinct subsets in an analysis of 249 cases. *Am J Surg Pathol* 2012;36:1592–608.
2 Pea A, Riva G, Bernasconi R, *et al*. Ampulla of Vater carcinoma: Molecular landscape and clinical implications. *World J Gastrointest Oncol* 2018;10:370–80.
3 Rostain F, Hamza S, Drouillard A, *et al*. Trends in incidence and management of cancer of the ampulla of Vater. *World J Gastroenterol* 2014;20:10144–50.
4 Shoji H, Morizane C, Hiraoka N, *et al*. Twenty-six cases of advanced ampullary adenocarcinoma treated with systemic chemotherapy. *Jpn J Clin Oncol* 2014;44:324–30.
5 Kim RD, Kundhal PS, McGilvray ID, *et al*. Predictors of failure after pancreaticoduodenectomy for ampullary carcinoma. *J Am Coll Surg* 2006;202:112–9.
6 Sikora SS, Balachandran P, Dimri K, *et al*. Adjuvant chemo-radiotherapy in ampullary cancers. *Eur J Surg Oncol* 2005;31:158–63.
7 Zhou J, Hsu CC, Winter JM, *et al*. Adjuvant chemoradiation versus surgery alone for adenocarcinoma of the ampulla of Vater. *Radiother Oncol* 2009;92:244–8.
8 Chang DK, Jamieson NB, Johns AL, *et al*. Histomolecular phenotypes and outcome in adenocarcinoma of the ampulla of vater. *J Clin Oncol* 2013;31:1348–56.
9 Yachida S, Wood LD, Suzuki M, *et al*. Genomic Sequencing Identifies ELF3 as a Driver of Ampullary Carcinoma. *Cancer Cell* 2016;29:229–40.
10 Hechtman JF, Liu W, Sadowska J, *et al*. Sequencing of 279 cancer genes in ampullary carcinoma reveals trends relating to histologic subtypes and frequent amplification and overexpression of ERBB2 (HER2). *Mod Pathol* 2015;28:1123–9.
11 Gingras M-C, Covington KR, Chang DK, *et al*. Ampullary Cancers Harbor ELF3 Tumor Suppressor Gene Mutations and Exhibit Frequent WNT Dysregulation. *Cell Rep* 2016;14:907–19.
12 Derksen PWB, Tjin E, Meijer HP, *et al*. Illegitimate WNT signaling promotes proliferation of multiple myeloma cells. *Proc Natl Acad Sci U S A* 2004;101:6122–7.
13 Kim JS, Crooks H, Foxworth A, *et al*. Proof-of-principle: oncogenic beta-catenin is a valid molecular target for the development of pharmacological inhibitors. *Mol Cancer Ther* 2002;1:1355–9.
14 Gunther EJ, Moody SE, Belka GK, *et al*. Impact of p53 loss on reversal and recurrence of conditional Wnt-induced tumorigenesis. *Genes Dev* 2003;17:488–501.
15 Alexandrov LB, Kim J, Haradhvala NJ, *et al*. The repertoire of mutational signatures in human cancer. *Nature New Biol* 2020;578:94–101.
16 Hsing AW, Gao Y-T, Han T-Q, *et al*. Gallstones and the risk of biliary tract cancer: a population-based study in China. *Br J Cancer* 2007;97:1577–82.
17 Andersen JB, Spee B, Blechacz BR, *et al*. Genomic and genetic characterization of cholangiocarcinoma identifies therapeutic targets for tyrosine kinase inhibitors. *Gastroenterology* 2012;142:1021–31.
18 Wimmer K, Kratz CP. Constitutional mismatch repair-deficiency syndrome. *Haematologica* 2010;95:699–701.
19 Lawrence MS, Stojanov P, Polak P, *et al*. Mutational heterogeneity in cancer and the search for new cancer-associated genes. *Nature New Biol* 2013;499:214–8.
20 Bailey MH, Tokheim C, Porta-Pardo E, *et al*. Comprehensive Characterization of Cancer Driver Genes and Mutations. *Cell* 2018;173:371–85.
21 Tsukiyama T, Fukui A, Terai S, *et al*. Molecular Role of RNF43 in Canonical and Noncanonical Wnt Signaling. *Mol Cell Biol* 2015;35:2007–23.
22 Chmielecki J, Hutchinson KE, Frampton GM, *et al*. Comprehensive genomic profiling of pancreatic acinar cell carcinomas identifies recurrent RAF fusions and frequent inactivation of DNA repair genes. *Cancer Discov* 2014;4:1398–405.
23 Alexandrov LB, Nik-Zainal S, Wedge DC, *et al*. Deciphering signatures of mutational processes operative in human cancer. *Cell Rep* 2013;3:246–59.
24 Pavlov YI, Shcherbakova PV, Rogozin IB. Roles of DNA polymerases in replication, repair, and recombination in eukaryotes. *Int Rev Cytol* 2006;255:41–132.
25 Jiang P, Gu S, Pan D, *et al*. Signatures of T cell dysfunction and exclusion predict cancer immunotherapy response. *Nat Med* 2018;24:1550–8.
26 Alexandrov LB, Jones PH, Wedge DC, *et al*. Clock-like mutational processes in human somatic cells. *Nat Genet* 2015;47:1402–7.
27 Jung H, Kim HS, Kim JY, *et al*. DNA methylation loss promotes immune evasion of tumours with high mutation and copy number load. *Nat Commun* 2019;10:4278.
28 Zhou W, Dinh HQ, Ramjan Z, *et al*. DNA methylation loss in late-replicating domains is linked to mitotic cell division. *Nat Genet* 2018;50:591–602.
29 Pinyol R, Sia D, Llovet JM. Immune Exclusion-Wnt/CTNNB1 Class Predicts Resistance to Immunotherapies in HCC. *Clin Cancer Res* 2019;25:2021–3.
30 Harding JJ, Nandakumar S, Armenia J, *et al*. Prospective Genotyping of Hepatocellular Carcinoma: Clinical Implications of Next-Generation Sequencing for Matching Patients to Targeted and Immune Therapies. *Clin Cancer Res* 2019;25:2116–26.
31 Spranger S, Bao R, Gajewski TF. Melanoma-intrinsic β-catenin signalling prevents anti-tumour immunity. *Nature New Biol* 2015;523:231–5.
32 Poulos RC, Olivier J, Wong JWH. The interaction between cytosine methylation and processes of DNA replication and repair shape the mutational landscape of cancer genomes. *Nucleic Acids Res* 2017;45:7786–95.
33 Rennoll S, Yochum G. Regulation of MYC gene expression by aberrant Wnt/β-catenin signaling in colorectal cancer. *World J Biol Chem* 2015;6:290–300.
34 Dang CV, O'Donnell KA, Zeller KI, *et al*. The c-Myc target gene network. *Semin Cancer Biol* 2006;16:253–64.
35 Poole CJ, van Riggelen J. MYC-Master Regulator of the Cancer Epigenome and Transcriptome. *Genes (Basel)* 2017;8:142.
36 Casey SC, Baylot V, Felsher DW. MYC: Master Regulator of Immune Privilege. *Trends Immunol* 2017;38:298–305.
37 Budczies J, Seidel A, Christopoulos P, *et al*. Integrated analysis of the immunological and genetic status in and across cancer types: impact of mutational signatures beyond tumor mutational burden. *Oncoimmunology* 2018;7:e1526613.
38 Faili A, Aoufouchi S, Weller S, *et al*. DNA polymerase eta is involved in hypermutation occurring during immunoglobulin class switch recombination. *J Exp Med* 2004;199:265–70.
39 Connor AA, Denroche RE, Jang GH, *et al*. Association of Distinct Mutational Signatures With Correlates of Increased Immune Activity in Pancreatic Ductal Adenocarcinoma. *JAMA Oncol* 2017;3:774–83.
40 Marnef A, Cohen S, Legube G. Transcription-Coupled DNA Double-Strand Break Repair: Active Genes Need Special Care. *J Mol Biol* 2017;429:1277–88.
41 Supek F, Lehner B. Clustered Mutation Signatures Reveal that Error-Prone DNA Repair Targets Mutations to Active Genes. *Cell* 2017;170:534–47.
42 Lanitis E, Dangaj D, Irving M, *et al*. Mechanisms regulating T-cell infiltration and activity in solid tumors. *Ann Oncol* 2017;28:xii18–32.
43 Krishnamurthy N, Kurzrock R. Targeting the Wnt/beta-catenin pathway in cancer: Update on effectors and inhibitors. *Cancer Treat Rev* 2018;62:50–60.
44 Emami KH, Nguyen C, Ma H, *et al*. A small molecule inhibitor of beta-catenin/CREB-binding protein transcription [corrected]. *Proc Natl Acad Sci U S A* 2004;101:12682–7.
45 Lepourcelet M, Chen Y-NP, France DS, *et al*. Small-molecule antagonists of the oncogenic Tcf/beta-catenin protein complex. *Cancer Cell* 2004;5:91–102.